of no help in determining the thermal or pressure history of a feldspar-bearing rock. However, it is possible that the pressure-induced monoclinic-to-triclinic transition interacts with the order-induced monoclinic-to-triclinic (orthoclase-to-microcline) transition. In this event pressure would enhance the formation of the triclinic ordered form. Furthermore, it is anticipated that partially ordered monoclinic feldspars will transform to triclinic symmetry at lower pressures than disordered feldspars of the same composition.

Perhaps the most intriguing aspect of this work is the evidence of possible isostructural *P-T-X* surfaces, and their close relationships to phase transition surfaces. The stability of many minerals is limited by geometrical packing limits of adjacent groups of polyhedra (such as micas, pyroxenes, amphiboles, and olivines). Since changes in temperature, pressure, and composition may all have the same effect of varying polyhedral size ratios (*9*), the concept of isostructural stability fields in *P-T-X* space does not seem unreasonable for these minerals. Of course, other phase regions will intersect the geometrically limiting surface. Still, the existence of isostructural *P-T-X* surfaces, and their close relationship to phase transition surfaces, may allow prediction of some phase equilibria from basic structural data.

ROBERT M. HAZEN*
Department of Mineralogy and Petrology, University of Cambridge, Cambridge CB2 3EW, England

References and Notes

1. J. V. Smith, *Feldspar Minerals* (Springer-Verlag, New York, 1974).
2. C. T. Prewitt, *Am. Mineral.*, in press.
3. Natural feldspars consist predominantly of three components: $NaAlSi_3O_8$ (albite), $KAlSi_3O_8$ (K-feldspar), and $CaAl_2Si_2O_8$ (anorthite). The composition of a given specimen is usually abbreviated $Or_xAb_yAn_z$ where *x*, *y*, and *z* give the mole percentages of the K-feldspar, albite, and anorthite components, respectively. In this report the use of Or_x alone implies the approximate composition Or_xAb_{1-x}.
4. Disordered feldspars at room temperature are metastable. Slow-cooled feldspars possess ordered Al-Si arrangements, while intermediate K/Na feldspars have the additional complication of exsolution of Na- and K-rich lamallae. High sanidines, in which there is complete Al-Si disorder and no exsolution, come from rapidly chilled volcanic rocks.
5. R. M. Hazen, thesis, Harvard University (1975).
6. W. MacKenzie, *Am. J. Sci.*, Bowen Volume, 319 (1952).
7. L. Merrill and W. A. Bassett, *Rev. Sci. Instrum.* **45**, 290 (1974).
8. R. M. Hazen and C. W. Burnham, *Am. Mineral.* **59**, 1166 (1974).
9. R. M. Hazen and C. T. Prewitt, in preparation.
10. P. J. Wyllie, *The Dynamic Earth* (Wiley, New York, 1971).
11. I thank J. D. C. McConnell, S. Agrell, A. Putnis, and C. T. Prewitt for their thoughtful reviews of the manuscript. Supported by a NATO Postdoctoral Fellowship in Science.
* Present address: Geophysical Laboratory, Carnegie Institution of Washington, 2801 Upton Street, NW, Washington, D.C. 20008.

16 June 1976; revised 23 July 1976

Jupiter's Spectrum Between 12 and 24 Micrometers

Abstract. *Spectroscopic measurements of the thermal radiation from Jupiter between 12 and 24 micrometers (420 to 840 reciprocal centimeters) with a resolution of 4 reciprocal centimeters are used to infer the Jovian temperature structure in the pressure region 0.1 to 0.4 atmosphere. The brightness temperature spectrum is in good agreement with previous ground-based measurements between 11 and 13 micrometers and with airborne measurements between 18 and 25 micrometers. However, the integrated flux calculated for a filter window and viewing angle equivalent to those of the 20 micrometer channel of Pioneer 10 is 20 percent below that measured by the Pioneer infrared radiometer. The Q branch of the ν_5 fundamental band of acetylene at 730 reciprocal centimeters appears in emission and leads to a mixing ratio estimate of $10^{-6 \pm 0.5}$.*

The spectrum of Jupiter between 12 and 24 μm is dominated by the $S(1)$ rotational line of the collisionally induced H_2 dipole, with a maximum opacity near 17 μm. We have observed Jupiter in this spectral region on 15 and 23 October 1975, using the 91-cm telescope of the G. P. Kuiper Airborne C141 Observatory operated at an altitude of 12,000 m. At this altitude the amount of CO_2 in the line of sight is reduced by nearly a factor of 7 compared to that at ground-based sites and, except for the region 14.3 to 15.9 μm, the brightness temperature spectrum of the region containing the center and the high- and low-frequency wings of the $S(1)$ line can be obtained with a single instrument. For wavelengths $\lambda < 13.8$ μm, ground-based measurements have been made by Gillett *et al.* (*1*) and Gillett (*2*) with a resolution of $\Delta\lambda/\lambda = 0.015$, by Aitken and Jones (*3*) with $\Delta\lambda/\lambda = 0.007$, by Ridgway (*4*) and Combes *et al.* (*5*) with a resolution of 1.3 cm^{-1} ($\Delta\lambda/\lambda \sim 0.0018$). For $\lambda > 18$ μm, aircraft measurements with $\Delta\lambda/\lambda = 0.03$ have been published by Houck *et al.* (*6*). In addition, the Pioneer 10 infrared radiometer has made broad-band (16 to 24 μm) radiance measurements from an aspect similar to that viewed from the earth, reported by Ingersoll *et al.* (*7*).

Our observations were made with a stepping Michelson interferometer using a KBr beam splitter and a Ge:Ga bolometer detector operated at 2°K. The instrument field of view was 36 arc seconds, while Jupiter subtended a mean diameter of 46 arc seconds. Telescope and sky background were canceled by oscillating the telescope secondary mirror between Jupiter and a point on the sky 3 arc minutes away at a rate of 28 hertz. The integrated signal from the residual background was less than 2 percent of the signal from Jupiter. Three spectra with a resolution of 1.95 cm^{-1} and nine spectra with a resolution of 3.9 cm^{-1} were obtained.

For absolute calibration, observations were made near the lunar limb (53° ± 5°N, 20° ± 8°W) in the vicinity of the crater Aristarchus, located in the northwest quadrant of Oceanus Procellarum. The solar meridian at the time of the observation was 49°W. For the emissivity and the temperature we have adopted $\epsilon = 0.90 \pm 0.05$ and $T = 394° \pm 7°$K, respectively, in the wavelength range of interest. The emissivity is based on a number of observations summarized by Linsky (*8*); the temperature was deduced from Apollo 17 observations by Low and Mendell (*9*), Apollo 17 heat flow experiments by Keihm and Langseth (*10*), and theoretical thermal response models by Schloerb and Muhleman (*11*).

Since here we are mainly concerned with the accurate definition of the continuum absolute brightness temperature spectrum, we present in the following the results of the analysis of the spectra obtained with a resolution of ~ 4 cm^{-1}. A more detailed description of the instrumentation, calibration methods, and analysis of the 2-cm^{-1} spectra will be presented elsewhere (*12*). The center line in Fig. 1 shows the calculated spectral brightness temperature of Jupiter (average of nine 4-cm^{-1} spectra, each requiring approximately 6 minutes of integration time) based on the lunar ratio spectrum, with $T_{moon} = 394$°K and $\epsilon_{moon} = 0.90$. No data are shown below 400 cm^{-1}, between 640 and 700 cm^{-1}, and above 850 cm^{-1}, where the combined system and atmospheric transmission drops below 20 percent of its maximum value. The brightness temperature increases at frequencies above and below the center of the $S(1)$ line at 587 cm^{-1}, indicating a rising temperature with depth, except for frequencies below 450 cm^{-1}, where the influence of the $S(0)$ rotational line near 350 cm^{-1} is observed. The relatively constant brightness temperature between 560 and 640 cm^{-1}, a region where the opacity significantly increases toward 600 cm^{-1}, indicates the presence of a level where the temperature is constant or increases with height.

The center line in Fig. 1 is bounded by the spectra representing ± 1 standard de-

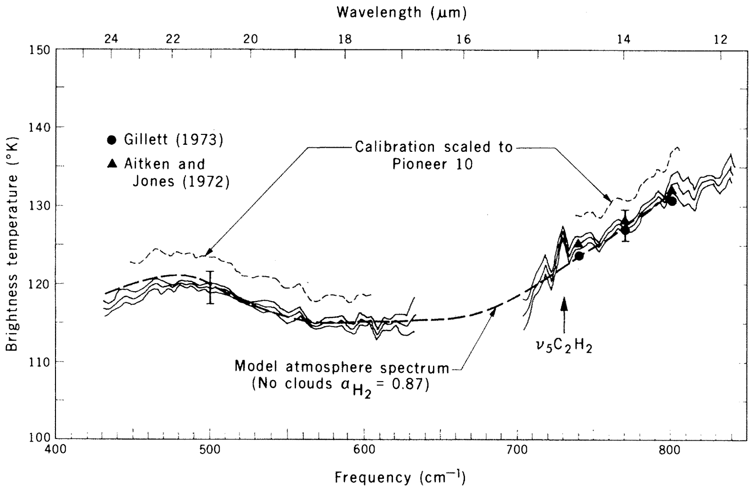

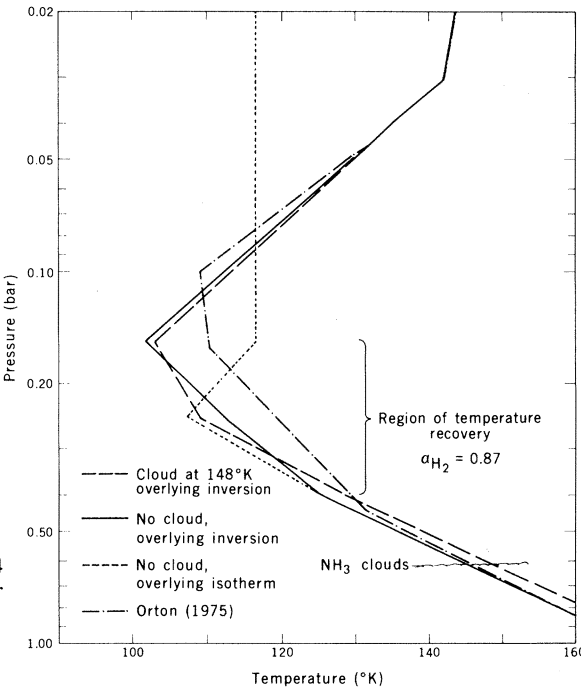

Fig. 1 (left). Brightness temperature spectrum of Jupiter between 12 and 24 μm. Fig. 2 (right). Mean Jovian thermal structure recovered from the October 1975 C141 spectrum and comparison with Pioneer 10 and ground-based results.

viation. Selected points from ground-based spectra (*2, 3*), shown near 12.5, 13, and 13.5 μm, agree within 0.5°K with this calibration. In the region 18 to 25 μm the calibration is in essential agreement with new Learjet data (*13*). The error bars shown at 13 and 20 μm reflect our absolute calibration uncertainty of ± 10 percent. The absorption feature at 23 μm and a small emission feature near 16 μm, reported in (*6*), are absent. The ν_5 *Q* branch of C_2H_2 at 730 cm^{-1} appears in emission, confirming the identification by Ridgway (*4*), based on *R*-branch observations, but is in some disagreement with the spectra reported by Combes *et al.* (*5*), where the emission feature associated with C_2H_2 appears at 765 cm^{-1}. The integrated flux, based on the nominal lunar calibration (T = 394°K and ϵ = 0.90), calculated for a filter window and viewing angle equivalent to those of the 20-μm channel of Pioneer 10, is 20 percent below that measured by the Pioneer infrared radiometer (*7*). The Pioneer data were averaged over zenith angles between 0° and 52°, as appropriate to our field of view. This disagreement is larger than our absolute calibration uncertainty. Uncertainties in centering the aperture on the planet should not result in serious errors in flux calibration since variations of the flux between center and limb are observed to be small near 20 μm (*14*). If our data were scaled to the 20-μm Pioneer 10 channel (thin dashed line in Fig. 1), they would raise the 13-μm brightness temperatures 3°K above those observed from the ground.

The mean Jovian temperature structure is quantitatively recovered from the data in a manner similar to that used by Orton (*14*). Information is obtained from six discrete central frequencies, representing data averaged over an 11.7-cm^{-1} interval. The averaging results in effective signal-to-noise ratios in the range of 35 to 100 for the representative data. In the computation of the H_2 dipole opacity the relative abundances of H_2 and He (by number) were assumed to be 0.87 and 0.13, respectively. These abundances are close to those expected from a "solar" mixture of elements and are in agreement with previously determined values (*6, 15*). For the effective signal-to-noise ratios, the temperature at three pressure levels, 0.16, 0.25, and 0.40 bar, may be determined independently. Below the deepest level (0.40 bar), an adiabatic lapse rate is assumed which is consistent with convective equilibrium. Above the highest level sounded (0.16 bar), two alternative assumptions are made. One is that the overlying structure is isothermal at the temperature of the 0.16-bar level. The other is that the overlying temperature structure is approximately that derived by Orton (*16*) from analysis of the Jovian spectrum near the 1306-cm^{-1} fundamental band of CH_4.

The temperature structure recovered with the isothermal assumption (short-dashed curve in Fig. 2) attempts to produce a thermal inversion region in order to match the flatness of the spectrum in the region 560 to 640 cm^{-1}. The isothermal assumption thus appears to be inappropriate. The structure recovered under the assumption of an overlying temperature inversion (solid curve in Fig. 2) reaches a minimum near 0.15 bar and drops at the adiabatic rate below 0.40 bar. This temperature structure is generally colder and approaches the adiabatic lapse rate at a considerably higher altitude in the atmosphere than the profile recovered from the spatially resolved broad-band measurements of Pioneer 10 and Pioneer 11 (*15*) (dash-dot curve in Fig. 2). This difference is clearly related to the 20 percent integrated flux disagreement in the 20-μm channel which was noted above, but for which we have at present no explanation. The effect of NH_3 clouds at the 148°K temperature level on the recovered mean temperature structure (long-dashed curve in Fig. 2) is relatively small.

The heavy dashed line in Fig. 1 shows the agreement between the observed and the calculated brightness temperature spectrum, based on the recovered vertical temperature structure, mixing ratios α_{H_2} = 0.87 and α_{He} = 0.13, and no minor constituents or clouds. The leveling off in the observed temperatures at frequencies above 800 cm^{-1} may be attributed to the wings of the ν_2 and $2\nu_2$ fundamental bands of NH_3. The small discrepancy at frequencies below 500 cm^{-1} could be caused by solid NH_3 haze, which has a broad absorption band near 400 cm^{-1} (*17*).

At 730 cm^{-1} a feature that rises above the level of observational uncertainty may be identified as the *Q* branch of the ν_5 fundamental band of C_2H_2, appearing in emission. A preliminary estimate of the abundance of this molecule, expressed as a constant mixing ratio, has been determined by including the C_2H_2 opacity in the synthetic spectrum calculation. The best fit corresponds to a mixing ratio of 10^{-6}, with an uncertainty of half an order of magnitude in either direction; the uncertainty is due to the use of a random band model in the opacity estimate and to the inability to fit the spectrum simultaneously in both Q and R branches of the ν_5 band. This abundance is essentially consistent with Strobel's photochemical models (*18*), but lower than Ridgway's (*4*) earlier estimate of 8×10^{-5}. Rigorous analysis awaits a more complete compilation of line positions and strengths in this band and comparison with detailed laboratory results. While Ridgway (*4*) also identified the ν_9 fundamental band of C_2H_6 near 820 cm^{-1}, we do not expect to be able to discriminate such an emission feature from our internal noise at a resolution of 4 cm^{-1}.

H. H. Aumann
G. S. Orton
Jet Propulsion Laboratory, California Institute of Technology, Pasadena 91103

References and Notes

1. F. C. Gillett, F. J. Low, W. A. Stein, *Astrophys. J.* **157**, 925 (1969).
2. F. C. Gillett, unpublished results.
3. D. K. Aitken and B. Jones, *Nature (London)* **240**, 230 (1972).
4. S. T. Ridgway, *Astrophys. J.* **187**, L41 (1974).
5. M. Combes, T. Encrenaz, L. Vapillon, Y. Zéau, *Astron. Astrophys.* **34**, 33 (1974).
6. J. R. Houck, J. B. Pollack, D. Schaack, R. A. Reed, A. Summers, *Science* **189**, 720 (1975).
7. A. P. Ingersoll, G. Münch, G. Neugebauer, G. S. Orton, in *Jupiter*, T. Gehrels, Ed. (Univ. of Arizona Press, Tucson, 1976), p. 197.
8. J. L. Linsky, *Astrophys. J.* **216** (Suppl. 1), 1 (1973).
9. F. J. Low and W. W. Mendell, *NASA Spec. Publ. SP330* **24**, 1 (1973).
10. S. J. Keihm and M. G. Langseth, Jr., in *Proceedings of the Fourth Lunar Science Conference*, W. A. Gose, Ed. (Pergamon, New York, 1974), vol. 3, p. 2503.
11. F. P. Schloerb and D. O. Muhleman, personal communication.
12. G. S. Orton and H. H. Aumann, in preparation.
13. R. A. Reed, personal communication.
14. G. S. Orton, *Icarus* **26**, 125 (1975).
15. ——— and A. P. Ingersoll, in *Jupiter*, T. Gehrels, Ed. (Univ. of Arizona Press, Tucson, 1976), p. 206.
16. G. S. Orton, *Icarus* **26**, 142 (1975).
17. F. W. Taylor, *J. Atmos. Sci.* **30**, 677 (1973).
18. D. F. Strobel, *Rev. Geophys. Space Phys.* **13**, 372 (1975).
19. We acknowledge helpful discussions with A. Ingersoll and the cooperation extended by the staff of the Airborne Science Office at NASA Ames and the C141 crew. This report presents results of research carried out at the Jet Propulsion Laboratory, California Institute of Technology, under NASA contract NAS 7-100. One of us (G.S.O.) is supported by a NASA-NRC Resident Research Associateship.

5 April 1976; revised 6 July 1976

Abnormal Visual Resolution in the Siamese Cat

Abstract. *When tested behaviorally, Siamese cats display marked differences in contrast sensitivity compared to ordinary cats. Overall sensitivity is depressed, the high-frequency cutoff point is lower, and there is less falloff in sensitivity at low spatial frequencies. Optical factors may contribute to these differences, or they may be attributable to the well-established anatomical abnormalities within the visual system of the Siamese cat.*

In the Siamese cat, optic fibers originating from about the first 20° of the temporal retina, just beyond the vertical midline, cross over to the contralateral side of the brain rather than remaining uncrossed as do most temporal fibers in the ordinary cat (*1*). As the result, subsequent stages in the visual pathways are confronted with an abnormally large contralateral input which the nervous system apparently deals with in one of several alternative ways (*2*). Because this congenital abnormality may disrupt the neuroanatomical substrate for normal vision, we and others have been interested in exploring behaviorally the possible visual consequences of this abnormality (*3*). During our work we unexpectedly discovered that Siamese cats suffer gross deficits in contrast sensitivity, a behavioral result which may reflect the existence of additional anamolies in the visual system of this albino mammal.

In our experiments, contrast thresholds were determined behaviorally with a conditioned suppression technique, the details of which are described elsewhere (*4, 5*). Cats were trained to lick a tube in order to obtain a small quantity of pureed beef, which was delivered on the average of once every ten licks. While licking, the cat faced an oscilloscope screen located 75 cm from its eyes. Conventional techniques (*6*) were used to generate on the screen either an uncontoured field of uniform luminance or vertical grating patterns of sinusoidal luminance profile; spatial frequency and contrast could be varied independently, and the grating and uncontoured display interchanged instantaneously, without altering the average luminance, which was 60 cd/m^2. The oscilloscope display and a restraining box which housed the cat were enclosed in a light-tight chamber; the cat was unobtrusively observed on a television monitor. During preliminary training, while the cat learned to lick, the oscilloscope display always was uncontoured. Once a stable lick rate was achieved, conditioned suppression trials were introduced. On these trials the uncontoured display was replaced for 15 seconds by a 0.5 cycle-per-degree grating of 0.45 contrast. The grating was turned off and on at the rate of 1.5 hertz, and at the end of the 15-second period a brief, unavoidable shock was delivered through the grid floor of the restraining box. Trials were initiated only when the cat was licking and appeared to be looking at the display. Once the cat was reliably suppressing to presentation of this high-contrast grating, we systematically varied contrast to find the value which produced a 50 percent reduction in lick rate, the conventional definition of threshold with this technique (*4*). Contrast thresholds were measured in this way over a range of spatial frequencies.

The results are shown in Fig. 1, with the open symbols plotting sensitivity (reciprocal of contrast threshold) of a typical ordinary cat and the filled symbols plotting sensitivity for two Siamese cats. Notice that at peak sensitivity (approximately 0.5 cycle per degree) the ordinary cat can detect a contrast of less than 1 percent, and that there is a reduction in sensitivity above and below this peak, with the high-frequency cutoff falling near 6 cycles per degree. This pattern of results is quite representative of ordinary cats: in our laboratory a total of six normal, adult cats have been tested for contrast sensitivity, and the same general curve is always found (cutoff frequency ranges from 4.7 to 6.5 cycles per degree). Using different techniques, others have reported much the same result (*7*). The contrast sensitivity functions for both Siamese cats, however, display several notable departures from the normal function: overall sensitivity is depressed by more than ½ log-unit at most points, the high-frequency cutoff is lower by at least a factor of 2, and there is little, if any, falloff in sensitivity at low spatial frequencies.

Like most Siamese cats, both the animals we tested displayed a noticeable convergent squint, which raises the possibility that the overall reduction in their contrast sensitivity could arise either from improper accommodation at a point nearer than the visual display or from some form of interocular suppression in response to diplopia. To test the first possibility, we reduced the viewing distance to 45 cm, by moving the oscilloscope toward the animal, and remeasured the contrast thresholds on one of the Siamese cats. This maneuver only served to pro-